

Spontaneous symmetry breaking of gap solitons in double-well traps

M. Trippenbach,¹ E. Infeld,² J. Gocąek,³ Michał Matuszewski,⁴ M. Oberthaler,⁵ and B. A. Malomed.⁶

¹*Institute of Theoretical Physics, Physics Department,
Warsaw University, Hoża 69, PL-00-681 Warsaw, Poland*

²*Soltan Institute for Nuclear Studies, Hoża 69, PL-00-681 Warsaw, Poland*

³*Institute of Physics, Polish Academy of Sciences, Al. Lotników 32/46, Warsaw, Poland*

⁴*Nonlinear Physics Center and ARC Center of Excellence for Quantum Atom Optics,
Research School of Physical Sciences and Engineering,*

Australian National University, Canberra ACT 0200, Australia

⁵*Kirchhoff-Institut für Physik, Im Neuenheimer Feld 227, 69120 Heidelberg, Germany*

⁶*Department of Interdisciplinary Sciences, School of Electrical Engineering,
Faculty of Engineering, Tel Aviv University, Tel Aviv 69978, Israel*

We introduce a two-dimensional model for the Bose-Einstein condensate with both attractive and repulsive nonlinearities. We assume a combination of a double-well potential in one direction, and an optical-lattice along the perpendicular coordinate. We look for dual-core solitons in this model, focusing on their symmetry-breaking bifurcations. The analysis employs a variational approximation, which is verified by numerical results. The bifurcation which transforms antisymmetric gap solitons into asymmetric ones is of supercritical type in the case of repulsion; in the attraction model, increase of the optical *lattice* strength leads to a gradual transition from subcritical bifurcation (for symmetric solitons) to a supercritical one.

PACS numbers: 03.75.Lm, 05.45.Yv, 42.65.Tg

I. INTRODUCTION

The Gross-Pitaevskii equation (GPE) provides a powerful model for studying the mean-field dynamics of Bose-Einstein condensates (BECs) [1]. Important examples are the prediction of 1D gap solitons (GSs) in a self-repulsive condensate trapped in a periodic optical-lattice (OL) potential [2]. This was realized experimentally in an ultracold gas of ⁸⁷Rb atoms confined in a cigar-shaped trap [3], and the prediction of the Josephson effect in a BEC [4]. It was subsequently observed in a condensate trapped in a macroscopic double-well potential [5]. In contrast to hitherto realized Josephson systems in superconductors and superfluids, interactions between tunneling particles play a crucial role in a bosonic junction. The effective nonlinearity induced by the interactions gives rise to new effects in the tunneling. In particular, anharmonic Josephson oscillations were predicted [6, 7, 8], provided that the initial population imbalance in the two potential wells falls below a critical value [9, 10]. This dynamic regime can be well explained by means of a simple model derived from the GPE, which amounts to a system of equations for the inter-well phase difference and population imbalance. The nonlinearity specific to the BEC also gives rise to a self-trapping effect in the form of a self-maintained population imbalance.

One-dimensional dynamics of a BEC in potentials composed of two rectangular potential wells were studied in several papers [11]. Stationary states with different populations in the two wells are generated by symmetry-breaking bifurcations from symmetric and antisymmetric states, for attractive and repulsive nonlinearity, respectively [9, 10]. A natural 2D extension of the double-well configuration is a *dual-channel* one, with the potential

featuring the two wells in the direction of x , which are extended into parallel troughs along the y axis [12, 13]. In the case of an attractive nonlinearity, this setting may naturally give rise to dual-core solitons, which are self-trapped in the y direction (similar to the ordinary matter-wave solitons created in a single-core trap [14]), and are supported by a double-well structure in the perpendicular direction. Furthermore, if the nonlinearity is strong enough, or else the tunnel coupling between the troughs is weak, the obvious symmetric dual-core soliton may bifurcate into an *asymmetric* one. This was demonstrated both in the full 2D model [12], and in its 1D counterpart, which replaces the 2D equation by a pair of one-dimensional GPEs with coordinate y , while the tunneling in the x direction is approximated by a linear coupling between the equations [13]. In fact, the latter model resembles the standard one widely accepted in nonlinear optics to describe dual-core nonlinear optical fibers and asymmetric solitons [15, 16]. In a similar way, the double-well potential may be uniformly extended in two transverse directions, giving rise to a 3D structure based on a pair of parallel “pancakes”.

If the dual-channel potential in 2D geometry is combined with an axial optical lattice, which runs along both potential troughs, it is natural to consider a dual-core gap soliton in the self-repulsive BEC filling this structure. In Ref. [13], this was done using the above-mentioned approximation which replaced the corresponding two-dimensional GPE by a pair of linearly-coupled 1D equations. It was demonstrated that a symmetric gap solitons may be stable in this case, and never bifurcate, while asymmetric solitons are generated by a symmetry-breaking bifurcation from antisymmetric ones. Similar results (including the emergence of asymmetric gap soli-

tons carrying intrinsic vorticity) were obtained in the 2D extension of the model. This model pertains to the above-mentioned “dual-pancake” structure [17]. In nonlinear optics, asymmetric gap solitons were studied in models of dual-core fiber Bragg gratings, which also amount to systems of linearly coupled 1D equations [18].

The prediction of symmetry breaking for matter-wave solitons in a setting combining the transverse double-well potential and a longitudinal optical lattice in experimentally relevant conditions makes it necessary to study the full 2D model (especially for the stability of the emerging asymmetric solitons) for both repulsive and attractive condensates, which is the purpose of the present work. Parameter regions admitting asymmetric solitons will be predicted by means of the variational approximation (VA) [16]. These results will be verified by numerics. The character of the symmetry-breaking bifurcations for the dual-core solitons will also be identified (we obtain a gradual transition from a subcritical bifurcation to a supercritical one with increase of the OL strength).

The paper is organized as follows. The model and the VA are introduced in Sec. II. In Sec. III we analyze the symmetry-breaking bifurcations in both attraction and repulsion models, and Sec. V concludes the paper.

II. THE MODEL AND VARIATIONAL APPROXIMATION

The normalized form of the GPE for the mean-field wave functions Ψ in 2D geometry is

$$i\Psi_t = -(1/2)(\Psi_{xx} + \Psi_{yy}) + [U(x) + \sigma|\Psi|^2 + \rho \cos(2y)]\Psi, \quad (1)$$

where $\sigma = +1$ and -1 for the self-repulsive and self-attractive BEC, and $\rho \cos(2y)$ represents the longitudinal optical lattice potential. The transverse double-well structure is taken as

$$U(x) = \begin{cases} 0, & |x| < L/2 \text{ and } |x| > L/2 + D, \\ -U_0, & L/2 < |x| < L/2 + D, \end{cases} \quad (2)$$

with D , U_0 and L being, respectively, the width and depth of each well, and the width of the barrier between them, see Fig. 1 below.

Stationary solutions to Eq. (1) are assumed in the form $\Psi(x, y, t) = e^{-i\mu t}\Phi(x, y)$, where the real function $\Phi(x, y)$ satisfies the equation

$$\mu\Phi + (1/2)(\Phi_{xx} + \Phi_{yy}) - U(x)\Phi - \sigma\Phi^3 + \rho \cos(2y)\Phi = 0. \quad (3)$$

It can be derived from the Lagrangian,

$$L_{\text{stat}} = \int \int dx dy [\mu\Phi^2 - (1/2)(\Phi_x^2 + \Phi_y^2) - U(x)\Phi^2 - (\sigma/2)\Phi^4 + \rho \cos(2y)\Phi^2]. \quad (4)$$

To apply the VA, we follow Ref. [12] and adopt an *ansatz* consisting of two distinct parts. First, inside each potential trough, i.e., at $|x \mp (L + D)/2| < D/2$, the trial

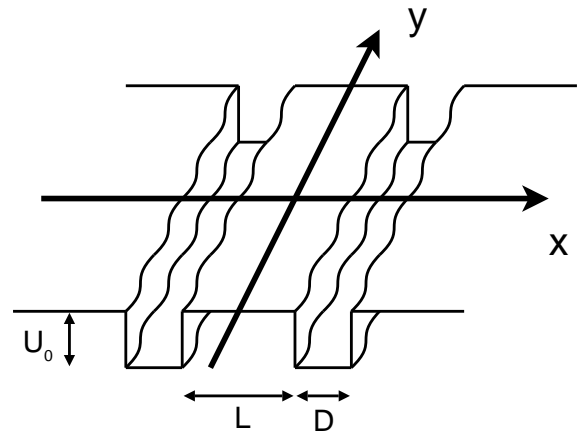


FIG. 1: (Color online) The shape of the quasi-one-dimensional double-well potential, $U(x, y)$. The wiggles indicate quasi-1D lattice along y .

function is

$$\Phi_{\pm}(x, y) = A_{\pm} \cos\left(\pi \frac{x \mp (L + D)/2}{D}\right) \exp\left(-\frac{y^2}{2W^2}\right), \quad (5)$$

where A_{\pm} and W are three variational parameters. This expression implies different amplitudes and a common longitudinal width, W , of the wave-function patterns in both troughs. In the x direction, the ansatz (5) emulates the ground-state wave function in an infinitely deep potential box, which vanishes at the edges of the trough, see Fig. 1. In the y direction, the ansatz approximates the self-trapped soliton by a Gaussian profile. Outside the troughs (at $|x| > L/2 + D$ and $|x| < L/2$), the ansatz also follows the pattern of quantum mechanics, in the form of a superposition of exponential wave functions:

$$\Phi(x, y) = \sum_{+,-} A_{\pm} \exp\left(-\sqrt{-2\mu} \left|x \mp \frac{L + D}{2}\right| - \frac{y^2}{2W^2}\right), \quad (6)$$

with the same amplitudes A_{\pm} and width W as in Eq. (5). The ansatz is not continuous at the edges of the troughs; however, comparison with numerical findings (see Fig. 2 below) clearly suggest that the VA can be used despite this local discrepancy.

Substitution of expressions (5) and (6) into Eq. (4) and integration produce the following simplified Lagrangian, in which contributions from the exponentially decaying functions in the outer region, $|x| > L/2 + D$, are neglected, the contribution from the optical lattice potential is taken into account only inside the troughs, and the Thomas-Fermi approximation in the x direction is adopted, i.e., term $-(1/2)\Phi_x^2$ in the Lagrangian density is omitted:

$$\frac{2}{D\sqrt{\pi}}L_{\text{eff}} = \frac{1}{2}\rho W e^{-W^2} (A_+^2 + A_-^2) \quad (7)$$

$$\begin{aligned}
& + \sum_{+,-} \left(\frac{\mu + U_0}{2} A_{\pm}^2 W - \frac{A_{\pm}^2}{8W} - \frac{3\sigma}{2^{9/2}} A_{\pm}^4 W \right) \\
& + \frac{4\sqrt{-2\mu}}{D} e^{-\sqrt{-2\mu}(L+D)} A_+ A_- W. \quad (8)
\end{aligned}$$

We now define $N_{\pm} \equiv (3/4\sqrt{2}) A_{\pm}^2 W$, and

$$\lambda \equiv (2/D) \sqrt{-2\mu} \exp\left(-\sqrt{-2\mu}(L+D)\right), \quad (9)$$

$$N \equiv \frac{N_+ + N_-}{4\sqrt{\lambda}}, \quad \nu \equiv \frac{N_+ - N_-}{4\sqrt{\lambda}}, \quad \epsilon \equiv \mu + U_0. \quad (10)$$

The numbers of atoms trapped in the two troughs are proportional to the respective partial norms of the wave function,

$$\left| \int_{-\infty}^{+\infty} dy \int_{\pm L/2}^{\pm(D+L/2)} dx (\Phi(x, y))^2 \right| = \frac{2\sqrt{2\pi}}{3} D N_{\pm}, \quad (11)$$

hence ν , defined in Eq. (10), measures the *population imbalance*. In this notation, the Lagrangian (8) simplifies to

$$\frac{3}{8\sqrt{2\pi}\lambda D} L_{\text{eff}} = \quad (12)$$

$$\equiv \frac{\epsilon N}{2} - \frac{N}{8W^2} - \sigma \frac{\sqrt{\lambda} N^2 + \nu^2}{2W} - s\lambda \sqrt{N^2 - \nu^2} + \frac{1}{2}\rho N e^{-W^2}, \quad (13)$$

with $s = +1$ and -1 for the configurations of the anti-symmetric and symmetric types (with $A_+ A_- < 0$ and $A_+ A_- > 0$, respectively).

Our Lagrangian gives rise to variational equations $\partial L/\partial W = \partial L/\partial \nu = \partial L/\partial N = 0$:

$$N + 2\sigma\sqrt{\lambda} (N^2 + \nu^2) W - 4\rho N W^4 e^{-W^2} = 0, \quad (14)$$

$$\nu \left(-\frac{\sigma}{W} + s\sqrt{\frac{\lambda}{N^2 - \nu^2}} \right) = 0, \quad (15)$$

$$\frac{1}{4W^2} + \sigma \frac{2\sqrt{\lambda} N}{W} + \frac{2s\lambda N}{\sqrt{N^2 - \nu^2}} - \rho e^{-W^2} = \epsilon. \quad (16)$$

Equation (15) has two solutions: $\nu = 0$, which corresponds to symmetric or antisymmetric solitons, and

$$\nu^2 = N^2 - \lambda W^2, \quad (17)$$

for asymmetric ones. Comparison of typical asymmetric and symmetric solitons, found from a numerical solution of Eq. (3), with their counterparts predicted by the VA, is presented in Fig. 2.

For symmetric and antisymmetric solitons, Eqs. (14) and (16), with $\nu = 0$, are tantamount to equations that were derived, by means of the VA, for solitons in 1D models with a periodic sinusoidal potential and attractive or repulsive nonlinearity [19, 20]. In particular, in the

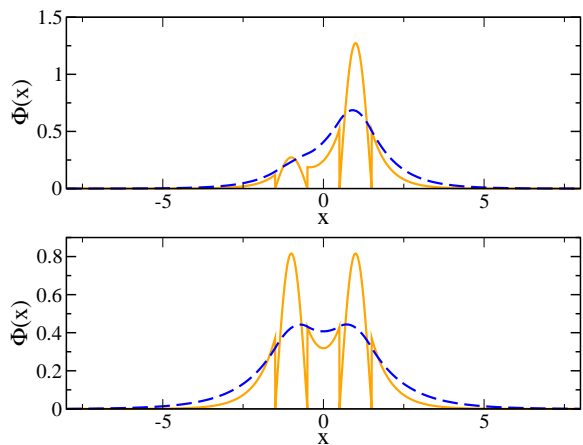


FIG. 2: (Color online) The top and bottom panels demonstrate examples of cross-section profiles, along $y = 0$, of stable asymmetric and symmetric gap solitons in the model with repulsion, as obtained from a numerical solution to Eq. (3) and predicted by the variational approximation (dashed and continuous lines, respectively). Parameters of the double-well potential are $L = D = 1$, $U_0 = -0.7$ (repulsive case) and $\rho = 1$. Norms of the asymmetric and symmetric solitons are, respectively, $N = 0.52$ and 0.34 . The asymmetry parameter for the former soliton, see Eqs. (10), is $\nu = 0.34$.

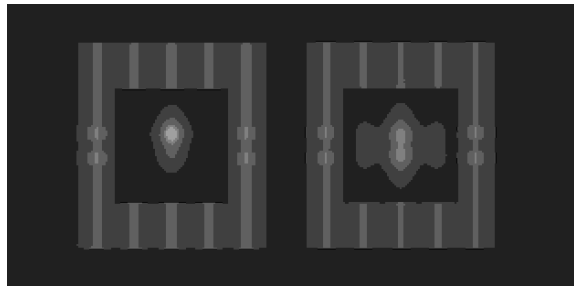


FIG. 3: Three dimensional version of the situation pictured in Fig. 2. The density scale is represented by the intensity of the print. Horizontal stripes represent double well structure and modulation illustrate the lattice

latter case (for $\sigma = +1$) a known fact is that solutions exist only for $\rho > \rho^{(0)} \equiv e^2/16 \approx 0.462$ (in fact, this constraint predicts, with high accuracy, the edge of the first finite bandgap in the linear spectrum induced by the OL [20]). Results for asymmetric solitons are presented in the next section.

III. ASYMMETRIC SOLUTIONS

A. Equations for the bifurcation point

According to Eq. (15), asymmetric solutions exist in two cases: $\sigma = s = +1$ (repulsion, with the asymmetric branch bifurcating from the antisymmetric one), or $\sigma = s = -1$ (attraction, with the bifurcation from the

symmetric branch). Elimination of ν^2 in Eqs. (14) and (16) by means of Eq. (17) yields a system of equations for N and W :

$$N + 2\sigma\sqrt{\lambda}W(2N^2 - \lambda W^2) = 4\rho NW^4 e^{-W^2}, \quad (18)$$

$$\frac{1}{4W^2} + \sigma\frac{2\sqrt{\lambda}N}{W} + \frac{2s\sqrt{\lambda}N}{W} - \rho e^{-W^2} = \epsilon.$$

Taking into account definitions (9) and (10), solutions to Eqs. (18) depend on parameters L, D, U_0 , and ρ .

At the bifurcation point, $\nu = 0$, Eq. (17) yields $N = \sqrt{\lambda}W$, hence Eqs. (17) generate a system of two equations for two coordinates of the bifurcation point, μ [via relations (10) and (9)] and W :

$$1 + 2\sigma\lambda W^2 = 4\rho W^4 e^{-W^2}, \quad (19)$$

$$\frac{1}{4W^2} + 2(\sigma + s)\lambda - \rho e^{-W^2} = \epsilon.$$

Without the OL, i.e., for $\rho = 0$ (the case considered in Ref. [12]), the first equation in (19) gives the bifurcation point at $N = 1/\sqrt{2}$. To obtain explicit results in the model with $\rho \neq 0$, one can start with an obvious solution to Eqs. (19), at $\lambda = \mu = N = 0$, $\rho = \rho^{(0)}$ (recall $\rho^{(0)} \equiv e^2/16$), $U = U_0^{(0)} \equiv 1/16$, and $W = W^{(0)} \equiv \sqrt{2}$. This solution, which has $N = 0$ is, by itself, trivial, but a nontrivial one can be obtained as an expansion around it.

B. The model with self-attraction

Consider the attraction model corresponding to $\sigma = s = -1$. Then, straightforward analysis of Eqs. (19) for small $\delta\rho = \rho - \rho^{(0)}$ and $\delta U_0 = U_0 - U_0^{(0)}$ demonstrates that the bifurcation of symmetric solitons (which pertain to $s = -1$, see above) may occur at two values of the norm,

$$N = \frac{1}{2\sqrt{2}} \sqrt{-(e^{-2}\delta\rho + \delta U_0)} \left[2 - \frac{1}{2} (e^{-2}\delta\rho + \delta U_0) \pm \sqrt{15e^{-2}\delta\rho - \delta U_0} \right], \quad (20)$$

the respective value of the width being $W \approx \sqrt{2} [1 - (e^{-2}\delta\rho + \delta U_0)/4]$. Note that the second term in the square brackets in Eq. (20) is a small correction to 2, the main correction given by the last term, which demonstrates that theoretically there may be two different bifurcation points. Obviously, expressions (20) are meaningful, i.e., the bifurcation takes place, if

$$(e^2/15)\delta U_0 < \delta\rho < -e^2\delta U_0 \quad (21)$$

(in other words, δU_0 must be negative, while $\delta\rho$ may have either sign). Numerical calculations imply that only the lower value of N is valid.

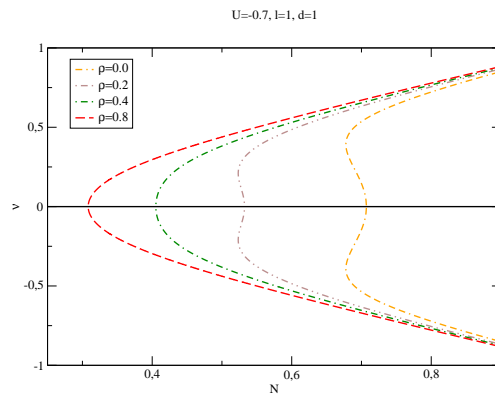


FIG. 4: (Color online) A set of numerically found bifurcation diagrams in the model with attraction, showing degree of a asymmetry of dual-core soliton, ν , as a function of the soliton's total norm, N , see Eqs. (10). The diagrams pertain to fixed values of parameters of the transverse double-well configuration, $L = D = 1$, $U_0 = -0.7$ (attractive case), while the strength of the longitudinal optical-lattice potential gradually increases. One can check from the analysis of Eq. (19) that the turning points are at $\nu = 0$ and $\pm N/\sqrt{3}$. One can clearly see that the supercritical bifurcation will turn into subcritical bifurcation with increase of the optical lattice strength.

A set of bifurcation diagrams in the attraction model, in the form of $\nu(N)$, i.e., curves showing the asymmetry of the dual-core solitons versus the total norm, was generated by a numerical solution of the full system of Eqs. (18). The set is displayed in Fig. 4, where a noteworthy feature is the transition from the *subcritical* shape (backward-directed one), which is a characteristic of the attraction model without the longitudinal OL [12] (as well as to the model of dual-core optical fibers [15]), to the simpler *supercritical* (forward-directed) shape at sufficiently large values of OL strength ρ . Note that the symmetry-breaking bifurcations of dual-core solitons, studied in systems of linearly-coupled GPEs including the attractive nonlinearity and OL potential [13, 17], as well as in the system of linearly-coupled fiber Bragg gratings [18], are of supercritical type too. The physical significance of the subcritical bifurcation is that it allows bistability of the solitons (the coexistence of stable symmetric and asymmetric ones) in a limited interval of values of N .

C. The model with self-repulsive nonlinearity

In the case of the self-repulsion, i.e., $\sigma = s = +1$, the expansion of Eqs. (19) predicts the following values of the norm at which asymmetric gap solitons may bifurcate from the antisymmetric ones (recall antisymmetric

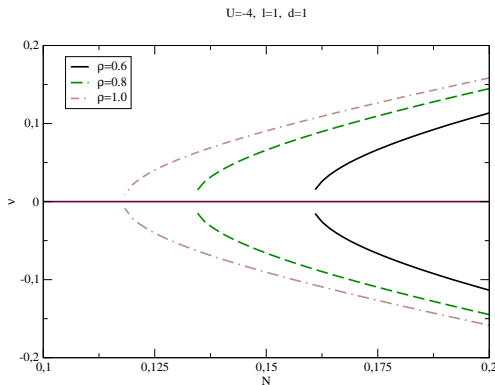


FIG. 5: (Color online) A set of bifurcation diagrams for gap solitons in the model with repulsive nonlinearity, for $L = D = 1$, $U_0 = 4$, and a set of different values of the OL strength, ρ .

solitons corresponds to $s = +1$):

$$N = \frac{1}{2\sqrt{2}} \sqrt{e^{-2}\delta\rho + \delta U_0} \left[2 - \frac{1}{2} (e^{-2}\delta\rho + \delta U_0) \pm \sqrt{15e^{-2}\delta\rho - \delta U_0} \right], \quad (22)$$

where the notation is the same as in Eq. (20) for the *attractive* model. This expression predicts the bifurcation in the following region [cf. Eq. (21) in the attraction model]: $-e^{-2}\delta\rho < \delta U_0 < 15e^{-2}\delta\rho$, which implies $\delta\rho > 0$, while δU_0 may be both positive and negative, in contrast with the case of the attraction model, that demanded $\delta U_0 < 0$, while allowing $\delta\rho$ to take either sign. Once again numerical calculations imply that only the lower value of N is valid.

A typical set of bifurcation diagrams in the repulsive model is displayed in Fig. 5. It is seen that the bifurcation generating asymmetric gap solitons from the antisymmetric ones is always of supercritical type, in com-

pliance with results obtained for the models based on linearly coupled GPEs with the optical lattice potential and repulsive nonlinearity [13, 17]. These bifurcation diagrams exist only for $\rho > \rho^{(0)} \equiv e^2/16$, because, as said above, at smaller values of the optical lattice strength the VA does not predict antisymmetric GSs that might give rise to a bifurcation.

IV. CONCLUSIONS

We have introduced a 2D model for self-attractive and self-repulsive BECs, which combines a double-well potential in the transverse direction, and a periodic potential along the longitudinal coordinate. The analysis involved symmetry-breaking bifurcations for dual-core solitons. Systematic results were obtained by means of the variational approximation, which was verified by numerical results. In the case of a repulsive nonlinearity, the bifurcation is of supercritical type, while in the model with attraction an increase of the optical lattice strength leads to a gradual transition from subcritical bifurcation to a supercritical one. This is an important result.

V. ACKNOWLEDGEMENTS

M.T. acknowledges the support of the Polish Government Research Grant for 2006-2009. E.I and M.M. acknowledges the support of the Polish Government Research Grant for 2007-2010 and 2007+2009. The work of B.A.M. was partially supported by the Israel Science Foundation through Excellence-Center grant No. 8006/03. He would like to thank Soltan Institute for Nuclear Studies, Warsaw, for an invitation in 2007. B.A.M. and M.O. acknowledge the support by German-Israel Foundation through grant No. 149/2006.

-
- [1] F. Dalfovo, S. Giorgini, L. P. Pitaevskii, and S. Stringari, *Rev. Mod. Phys.* **71**, 463 (1999).
 - [2] F. Kh. Abdullaev *et al.*, *Phys. Rev. A* **64**, 043606 (2001); I. Carusotto, D. Embriaco, and G. C. La Rocca, *ibid.* **65**, 053611 (2002); B. B. Baizakov, V. V. Konotop and M. Salerno, *J. Phys. B* **35**, 5105 (2002); E. A. Ostrovskaya and Y. S. Kivshar, *Phys. Rev. Lett.* **90**, 160407 (2003); *Opt. Exp.* **12**, 19 (2004).
 - [3] B. Eiermann *et al.*, *Phys. Rev. Lett.* **92**, 230401 (2004).
 - [4] J. Javanainen, *Phys. Rev. Lett.* **57**, 3164 (1986); A. Smerzi *et al.*, *Phys. Rev. Lett.* **79**, 4950 (1997); S. Raghavan *et al.*, *Phys. Rev. A* **59**, 620 (1999); S. Giovanazzi, A. Smerzi, and S. Fantoni, *Phys. Rev. Lett.* **84**, 4521 (2000); E. A. Ostrovskaya *et al.*, *Phys. Rev. A* **61**, 031601(R) (2000); K. W. Mahmud, J. N. Kutz, and W. P. Reinhardt, *Phys. Rev. A* **66**, 063607 (2002).
 - [5] M. Albiez *et al.*, *Phys. Rev. Lett.* **95**, 010402, (2005).
 - [6] J. Javanainen, *Phys. Rev. Lett.* **57**, 3164 (1986).
 - [7] M. W. Jack, M. J. Collett, and D. F. Walls, *Phys. Rev. A* **54**, R4625 (1996).
 - [8] I. Zapata, F. Sols, and A. J. Leggett, *Phys. Rev. A* **57**, R28 (1998).
 - [9] G. J. Milburn, J. Corney, E. M. Wright, and D. F. Walls, *Phys. Rev. A* **55**, 4318 (1997).
 - [10] A. Smerzi *et al.*, *Phys. Rev. Lett.* **79**, 4950 (1997); S. Raghavan *et al.*, *Phys. Rev. A* **59**, 620 (1999).
 - [11] P. Zin *et al.*, *Phys. Rev. A* **73**, 022105 (2006), E. Infeld *et al.*, *Phys. Rev. E* **74**, 026610 (2006); for a review, see R. Gati and M. Oberthaler, *J. Phys. B.* **40**, R61 (2007).
 - [12] M. Matuszewski, B. A. Malomed, and M. Trippenbach, *Phys. Rev. A* **75**, 063621 (2007).
 - [13] A. Gubeskys and B. A. Malomed, *Phys. Rev. A* **75**, 063602 (2007).
 - [14] K. E. Strecker *et al.*, *Nature* **417**, 150 (2002); L. Khaykovich *et al.*, *Science* **256**, 1290 (2002).
 - [15] E. M. Wright, G. I. Stegeman, and S. Wabnitz, *Phys.*

- Rev. A **40**, 4455 (1989); N. Akhmediev and A. Ankiewicz, Phys. Rev. Lett. **70**, 2395 (1993); P. L. Chu, B. A. Malomed, and G. D. Peng, J. Opt. Soc. Am. B **10**, 1379 (1993).
- [16] V. M. Pérez-García *et al.*, Phys. Rev. A **56**, 1424 (1997); B. A. Malomed, in: *Progress in Optics*, vol. **43**, p. 71 (ed. by E. Wolf: North Holland, Amsterdam, 2002).
- [17] A. Gubeskys and B. A. Malomed, Phys. Rev. A **76**, 043623 (2007).
- [18] W. Mak, B. A. Malomed, and P. L. Chu, J. Opt. Soc. Am. B **15**, 1685 (1998); Y. J. Tsofe and B. A. Malomed, Phys. Rev. E **75**, 056603 (2007).
- [19] B. A. Malomed, Z. H. Wang, P. L. Chu, and G. D. Peng, J. Opt. Soc. Am. B **16**, 1197 (1999).
- [20] S. Adhikari and B. A. Malomed, Europhys. Lett. **79**, 50003 (2007); Phys. Rev. A **76**, 043626 (2007).